

# Synthesis and Solution State Characterization by Gradient-Enhanced 2D Multinuclear NMR Spectroscopy of a Fluorine-Bridged Dimethyltin(IV) Salicylaldoximate Derivative

Abdelkrim Meddour,<sup>†,‡</sup> Frédéric Mercier,<sup>†,§</sup> José C. Martins,<sup>†</sup> Marcel Gielen,<sup>§</sup>  
Monique Biesemans,<sup>†,§</sup> and Rudolph Willem<sup>\*,†,§</sup>

High Resolution NMR Centre (HNMR) and Laboratory of General and Organic Chemistry of the Faculty of Applied Sciences (AOSC), Free University of Brussels (VUB), Pleinlaan 2, B-1050 Brussel, Belgium

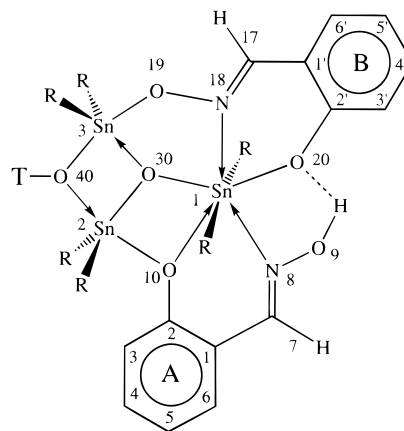
Received July 9, 1997<sup>⊗</sup>

The reaction of [(Me<sub>2</sub>Sn)<sub>2</sub>(Me<sub>2</sub>SnO)(ONZOH)(HONZO)(ONZO)] (HONZOH = *o*-HON=CHC<sub>6</sub>H<sub>4</sub>OH, salicylaldoxime) with ammonium fluoride yields a fluorotris(dimethyltin) disalicylaldoximate complex, compound **4**, containing one seven-coordinate and two five-coordinate tin atoms, with a fluoride anion bridging the five-coordinate tin atoms. Though **4** can be obtained in a crystalline form, its crystals are unsuitable for X-ray analysis. Its structure has been completely characterized in solution by 1D <sup>1</sup>H, <sup>13</sup>C, <sup>119</sup>Sn, and <sup>19</sup>F NMR spectra and 2D gradient-assisted <sup>1</sup>H–<sup>119</sup>Sn and <sup>1</sup>H–<sup>13</sup>C HMQC and HMBC NMR spectra. In solution, **4** is involved in an equilibrium with several species. It is shown that the Sn(2)–F–Sn(3) moiety of **4** is the reactive site amenable to nucleophilic substitution with weak nucleophiles like water and methanol. The preservation of the splitting of the <sup>1</sup>J(<sup>119/117</sup>Sn(3)–<sup>19</sup>F) coupling but not the <sup>1</sup>J(<sup>119/117</sup>Sn(2)–<sup>19</sup>F) coupling evidences a reaction intermediate where the entering nucleophile is bound to the Sn(2) tin atom whereas the fluoride is still linked to the Sn(3) atom. Overall,  $\mu_2$ -nucleophilic substitutions on compound **4** with hydroxylated nucleophiles should be viewed as addition–elimination reactions.

## Introduction

Condensation compounds obtained from salicylaldoxime *o*-HON=CHC<sub>6</sub>H<sub>4</sub>OH and diorganotin(IV) oxide, R<sub>2</sub>SnO (R = Me, *n*-Bu), are small clusters represented as [(R<sub>2</sub>Sn)<sub>2</sub>(R<sub>2</sub>SnO)(ONZOH)(HONZO)(ONZO)] (**1b**, R = *n*-Bu; **2b**, R = Me), where ONZOH is the monobasic species *o*-(<sup>-</sup>ON=CHC<sub>6</sub>H<sub>4</sub>OH), HONZO is the phenolate *o*-HON=CHC<sub>6</sub>H<sub>4</sub>O<sup>-</sup>, and ONZO is the dibasic species *o*-(<sup>-</sup>ON=CHC<sub>6</sub>H<sub>4</sub>O<sup>-</sup>) associated with salicylaldoxime.<sup>1</sup> Their structure consists of three unequivalent diorganotin(IV) moieties, one dibasic and two monobasic salicylaldoximate units involved in a network of tin–oxygen and tin–nitrogen bonds with one seven-coordinate and two five-coordinate tin atoms (Figure 1).<sup>1</sup>

Recrystallization of crude **1b** (R = *n*-Bu) in hexane, acetonitrile, or methanol did not afford crystals of **1b** but of **1a**, a compound where the  $\mu_2$ -salicylaldoximate ONZOH unit is substituted for a  $\mu_2$ -OH group bridging the Sn(2) and Sn(3) atoms.<sup>1a</sup> Similarly, attempts to recrystallize **2b** (R = Me) from low molecular weight alcohols failed and resulted instead in the generation of new crystalline compounds that had the same core as **2b** but where the  $\mu_2$ -salicylaldoximate ONZOH unit was substituted for a  $\mu_2$ -alkoxy bridging group as, e.g., **3** for T = Me, [(R<sub>2</sub>Sn)<sub>2</sub>(R<sub>2</sub>SnO)(OMe)(ONZO)(HONZO)].<sup>1b</sup> These reactions are summarized in Scheme 1.



	T	R
<b>1a</b>	H	<i>n</i> -Bu
<b>1b</b>	HOZN	<i>n</i> -Bu
<b>2a</b>	H	Me
<b>2b</b>	HOZN	Me
<b>3</b>	Me	Me

**Figure 1.** General structure, with atom labeling, of compounds from several condensation reactions between di-*n*-butyl- or dimethyltin(IV) oxide and salicylaldoxime, synthesized previously (**1a**, **1b**;<sup>1a</sup> **2b**, **3a**–**e**<sup>1b</sup>). HOZN represents the salicylaldoximate residue bound to O(40) by its nitrogen atom.

Reactions of **3** with various nucleophiles having a weak acidic character like phenols have been studied.<sup>2</sup> All nucleophiles considered so far led to the substitution of the  $\mu_2$ -O–T unit for

\* Corresponding author. E-mail: rwillem@vub.ac.be.

<sup>†</sup> High Resolution NMR Centre.

<sup>‡</sup> On leave from the Laboratoire de Chimie Structurale Organique, Université de Paris-Sud, Bât. 410, ICMO, CNRS URA No.1384, 91405 Orsay Cedex, France.

<sup>§</sup> Laboratory of General and Organic Chemistry.

<sup>⊗</sup> Abstract published in *Advance ACS Abstracts*, November 1, 1997.

(1) (a) Kayser, F.; Biesemans, M.; Bouâlam, M.; Tiekink, E. R. T.; El Khloufi, A.; Meunier-Piret, J.; Bouhdid, A.; Jurkschat, K.; Gielen, M.; Willem, R. *Organometallics* **1994**, *13*, 1098 and 4126. (b) Willem, R.; Bouhdid, A.; Kayser, F.; Delmotte, A.; Gielen, M.; Martins, J. C.; Biesemans, M.; Mahieu, B.; Tiekink, E. R. T. *Organometallics* **1996**, *15*, 1920.

(2) Willem, R.; Bouhdid, A.; Meddour, A.; Camacho-Camacho, C.; Mercier, F.; Gielen, M.; Biesemans, M.; Ribot, F.; Sanchez, C.; Tiekink, E. R. T. *Organometallics* **1997**, *16*, 4377.

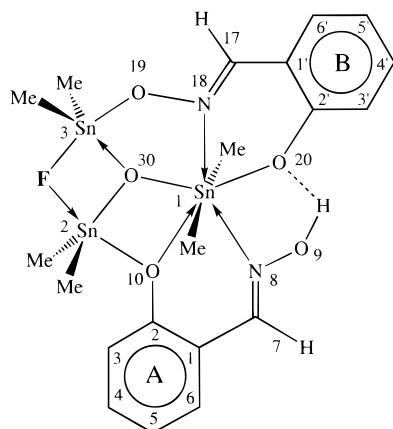
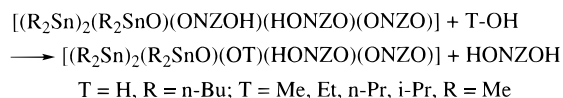


Figure 2. Solution structure of **4**.

### Scheme 1



another one bridging the Sn(2) and Sn(3) atoms. The purpose of this report is to find out whether such a bridging is only due to the great oxophilicity of tin atoms or, instead, whether substitution is also possible with a weaker nucleophile bearing no oxygen atom. More specifically, as  $\mu_2$ -bridging properties of the fluoride anion have been known for some time in organotin fluorides,<sup>3</sup> we aimed at examining whether reaction of **2b** or **3** with ammonium fluoride can provide such a cluster with a bridging fluoride.

The present study reports structural investigations in solution by 1D and 2D NMR spectroscopy, mainly gradient-assisted<sup>4</sup>  $^1H$ - $^{13}C$  HMQC<sup>5a</sup> and HMBc<sup>5b,c</sup> and  $^1H$ - $^{119}Sn$  HMQC,<sup>6</sup> on the novel compound  $[(R_2Sn)_2(R_2SnO)(F)(ONZO)(HONZO)]$ , **4** (Figure 2).

### Results and Discussion

**Synthesis.** In previous studies, nucleophilic substitutions were achieved either by reacting **2b** with the alcohol from which the substitution product subsequently crystallizes<sup>1</sup> or by an equilibrium shift of **3** in the presence of the entering nucleophile, followed by crystallization in benzene-hexane or dichloromethane-hexane to yield the desired product.<sup>2</sup> Here, the fluorine-bridged complex **4** has been prepared by reacting **2b** with ammonium fluoride in dichloromethane, followed by a tedious multistep purification.

The reaction of **2b** with 1.2 equiv of ammonium fluoride leads, after filtration of unreacted  $NH_4F$ , to an equilibrium

mixture composed of **4**, **2b**, and salicylaldoxime in an approximate molar ratio 2/1/2. Due to the relatively high solubility of **4** in usual solvents and to the presence of salicylaldoxime in the reaction medium, no crystallization of crude **4** by slow evaporation of the solvent is possible, an oil being unavoidably obtained. Similarly, attempts to use a binary solvent to selectively precipitate **4** or salicylaldoxime failed. The final separation procedure exploited the difference in solubility of the three reaction mixture components in refluxing and cold hexane. When the mixture is refluxed in hexane, **2b** precipitates. After filtration, followed by evaporation of the major part of the solvent, an oil mainly composed of salicylaldoxime separates from the mixture upon cooling to room temperature. After elimination of the latter, cooling further the remaining solution allows the precipitation of a solid, which is subsequently recrystallized in hexane to yield pure crystals of **4**.

**Solution State Structure.** The crystals of **4** obtained from several crystallizations were unsuitable for X-ray analysis. Consequently, the structural characterization of **4** was achieved only in solution using 1D and 2D NMR spectroscopy in  $C_6D_6$ . As for other diorganotin salicylaldoximate complexes,<sup>1,2</sup> dissolution of **4** causes the appearance of minor species, among which are **2a** and **2b**. Nevertheless, **4** remains the major species in solution (83% of the total  $^{119}Sn$  NMR signal).

Table 1 presents an overview of the  $^1H$ ,  $^{13}C$ ,  $^{19}F$ , and  $^{119}Sn$  chemical shifts and coupling constants associated with the dimethyltin moieties. The  $^1H$ ,  $^{13}C$ , and  $^{119}Sn$  resonances were assigned with exactly the same strategy reported previously for **2b** and **3** using 2D gradient-enhanced  $^1H$ - $^{13}C$  HMQC and HMBC spectroscopy<sup>1,2</sup> and  $^1H$ - $^{119}Sn$  HMQC spectroscopy. They evidence that **4** has the same basic tritin cluster structure as **2b** and **3** with one seven-coordinate and two five-coordinate tin atoms and two nonequivalent salicylaldoximate ligands (Figure 2). The  $^1H$ - $^{119}Sn$  HMQC cross-peaks of **4**, reviewed in Table 2, similar to those of **1a**, **1b**, **2a**, **2b**, and **3**, support this analysis, as do all the  $^1J(^{13}C-^{119/117}Sn)$ ,  $^nJ(^{119}Sn-O-^{119/117}Sn)$ , and  $^2J(^1H-^{119/117}Sn)$  coupling data. That the fluoride anion bridges the two five-coordinate atoms, Sn(2) and Sn(3), and therefore that **4** results from a substitution of the  $\mu_2$ -linked ONZO moiety for a  $\mu_2$ -linked F anion is demonstrated by the following special  $^nJ(^{119}Sn-^{19}F)$  coupling features. The  $^{119}Sn$  resonances are doublets centered at -105.7, -120.3, and -444.6 ppm for Sn(3), Sn(2), and Sn(1), respectively, with  $^1J(^{119}Sn-^{19}F)$  coupling constant values of 1271 and 1285 Hz for Sn(3) and Sn(2), respectively, and a smaller  $^3J(^{119}Sn-^{19}F)$  splitting of 65 Hz for Sn(1). The  $^1J(^{119}Sn-^{19}F)$  couplings for Sn(2) and Sn(3), mutually of the same order of magnitude but smaller than  $^1J(^{119}Sn-^{19}F)$  values, in the range 1500-3400 Hz for standard Sn-F bonds,<sup>7</sup> unambiguously reveal a fluorine atom bridging the Sn(2) and Sn(3) atoms. The slight nonequivalence of the  $^1J(^{119}Sn(2)-^{19}F)$  and the  $^1J(^{119}Sn(3)-^{19}F)$  coupling constants is in agreement with the chemical nonequivalence of the two Sn-F bonds.

The  $^{19}F$  NMR spectrum confirms this proposal, since it displays a single central resonance at -83.9 ppm with five

- (3) Dakternieks, D.; Jurkschat, K.; Zhu, H.; Tiekink, E. R. T. *Organometallics* **1995**, *14*, 2512.  
 (4) (a) Keeler, J.; Clowes, R. T.; Davis, A. L.; Laue, E. D. *Methods Enzymol.* **1994**, *239*, 145. (b) Tyburn, J.-M.; Bereton, I. M.; Doddrell, D. M. *J. Magn. Reson.* **1992**, *97*, 305. (c) Ruiz-Cabello, J.; Vuister, G. W.; Moonen, C. T. W.; Van Gelderen, P.; Cohen, J. S.; Van Zijl, P. C. M. *J. Magn. Reson.* **1992**, *100*, 282. (d) Vuister, G. W.; Boelens, R.; Kaptein, R.; Hurd, R. E.; John, B. K.; Van Zijl, P. C. M. *J. Am. Chem. Soc.* **1991**, *113*, 9688.  
 (5) (a) Bax, A.; Griffey, R. H.; Hawkins, B. L. *J. Magn. Reson.* **1983**, *55*, 301. (b) Bax, A.; Summers, M. F. *J. Am. Chem. Soc.* **1986**, *108*, 2093. (c) Bax, A.; Summers, M. F. *J. Magn. Reson.* **1986**, *67*, 565.  
 (6) (a) Kayser, F.; Biesemans, M.; Gielen, M.; Willem, R. *J. Magn. Reson.* **1993**, *A102*, 249. (b) Martins, J. C.; Verheyden, P.; Kayser, F.; Gielen, M.; Willem, R.; Biesemans, M. *J. Magn. Reson.* **1997**, *124*, 218. (c) Kayser, F.; Biesemans, M.; Gielen, M.; Willem, R. In *Advanced Applications of NMR to Organometallic Chemistry*; Gielen, M., Willem, R., Wrackmeyer, B., Eds.; Wiley: Chichester, U.K., 1996; Chapter 3, pp 45-86.

- (7) (a) Wrackmeyer, B. *Annu. Rep. NMR Spectrosc.* **1985**, *16*, 73. (b) Al-Juaid, S.; Dhaher, S. M.; Eaborn, C.; Hitchcock, P. B.; Smith, J. D. *J. Organomet. Chem.* **1987**, *325*, 117. (c) Reuter, H.; Puff, H. *J. Organomet. Chem.* **1989**, *379*, 223. (d) Dakternieks, D.; Zhu, H. *Organometallics* **1992**, *11*, 3820. (e) Dostal, S.; Stoudt, S. J.; Fanwick, P.; Sereaton, W. F.; Kahr, B.; Jackson, J. E. *Organometallics* **1993**, *12*, 2284. (f) Kolb, U.; Dräger, M.; Dargatz, M.; Jurkschat, K. *Organometallics* **1995**, *14*, 2827. (g) Preut, H.; Godry, B.; Mitchell, T. N. *Acta Crystallogr.* **1992**, *C48*, 1994. (h) Ochiai, M.; Iwaki, S.; Ukita, T.; Matsuura, Y.; Shiro, M.; Nagao, Y. *J. Am. Chem. Soc.* **1988**, *110*, 4606. (i) Pieper, N.; Klaus-Mrestani, C.; Schürmann, M.; Jurkschat, K.; Biesemans, M.; Verbruggen, I.; Martins, J. C.; Willem, R. *Organometallics* **1997**, *16*, 1043.

**Table 1.**  $^{119}\text{Sn}$ ,  $^{13}\text{C}$ , and  $^1\text{H}$  NMR Data for the Dimethyltin Moiety of **4**<sup>a</sup> in  $\text{C}_6\text{D}_6$  Solution

moiety	$\delta(^{119}\text{Sn})$	$^nJ(^{119}\text{Sn}-^{119/117}\text{Sn})$	$^nJ(^{19}\text{F}-^{119/117}\text{Sn})$	$\delta(^{13}\text{C})$	$^1J(^{13}\text{C}-^{119/117}\text{Sn})$	$\delta(^1\text{H})$	$^2J(^1\text{H}-^{119/117}\text{Sn})$
$\text{Me}_2\text{Sn}(1)$	-444.6	322 <sup>b</sup>	65/62 <sup>c</sup>	14.8	1095/1046	1.07	112.2/107.3
$\text{Me}_2\text{Sn}(2)$	-120.3	42, <sup>b</sup> 42 <sup>b</sup>	1285/1228 <sup>d</sup>	2.9	662 <sup>e</sup>	0.60	77.7/74.4
$\text{Me}_2\text{Sn}(3)$	-105.7	329/315, 41 <sup>b</sup>	1271/1215 <sup>d</sup>	0.9	636 <sup>e</sup>	0.55	78.5/75.1

<sup>a</sup> Chemical shift data in ppm and coupling constants in Hz. <sup>b</sup> Averaged values from unresolved  $^nJ(^{119}\text{Sn}-^{119}\text{Sn})$  and  $^nJ(^{119}\text{Sn}-^{117}\text{Sn})$  coupling satellites in  $^{119}\text{Sn}$  spectrum as assessed by simulation. The corresponding satellites at the  $^{119}\text{Sn}(1)$  resonance are invisible because of the broad signal feet. <sup>c</sup>  $^3J(^{19}\text{F}-^{117}\text{Sn})$  coupling constant calculated from  $^3J(^{19}\text{F}-^{119}\text{Sn})$ . <sup>d</sup>  $^1J(^{19}\text{F}-^{119}\text{Sn})/^1J(^{19}\text{F}-^{117}\text{Sn})$ . <sup>e</sup> Averaged values from unresolved  $^1J(^{13}\text{C}-^{119}\text{Sn})$  and  $^1J(^{13}\text{C}-^{117}\text{Sn})$  coupling satellites in the  $^{13}\text{C}$  spectrum.

**Table 2.**  $^1\text{H}-^{119}\text{Sn}$  Correlation Data As Obtained from 2D  $^1\text{H}-^{119}\text{Sn}$  HMQC and 1D  $^1\text{H}$  NMR Spectra Recorded from a  $\text{C}_6\text{D}_6$  Solution of **4**<sup>a</sup>

tin atom	$\delta(^{119}\text{Sn})^b$	oximic protons	other protons <sup>b</sup>
Sn(1)	-444.6	H(17): 8.17, $^3J = 4.9$ H(7): 8.10, $^3J = 11.8$	H(9): 13.55, $^3J = 4.2$ CH <sub>3</sub> <sup>c</sup> : 1.07, $^2J = 112.2$ CH <sub>3</sub> -Sn(2): 0.60, $^4J < 2$ CH <sub>3</sub> -Sn(3): 0.55, $^4J < 2$
Sn(2)	-120.3	H(17): 8.17, $^5J < 2$	H(6): 6.80 (weak) H(5): 6.60-6.53 (weak) H(3): 6.12, $^4J = 13.6$ CH <sub>3</sub> -Sn(1): 1.07, $^4J < 2$ CH <sub>3</sub> <sup>c</sup> : 0.60, $^2J = 77.7$
Sn(3)	-105.7	H(17): 8.17, $^4J < 2$	CH <sub>3</sub> -Sn(1): 1.07, $^4J < 2$ CH <sub>3</sub> <sup>c</sup> : 0.55, $^2J = 78.3$

<sup>a</sup>  $^1\text{H}$  chemical shift and  $^nJ(^1\text{H}-^{119}\text{Sn})$  are given for each proton that correlates with a  $^{119}\text{Sn}$  resonance (see Figure 2 for labeling). <sup>b</sup> Chemical shifts are given in ppm and coupling constants in Hz. <sup>c</sup> Methyl group bound to the considered tin atom.

satellite splittings of 1285, 1272, 1228, 1215, and 65 Hz assigned to scalar couplings between the unique  $^{19}\text{F}$  nucleus and the  $^{119}\text{Sn}(2)$ ,  $^{119}\text{Sn}(3)$ ,  $^{117}\text{Sn}(2)$ ,  $^{117}\text{Sn}(3)$ , and  $^{119/117}\text{Sn}(1)$  nuclei, respectively.

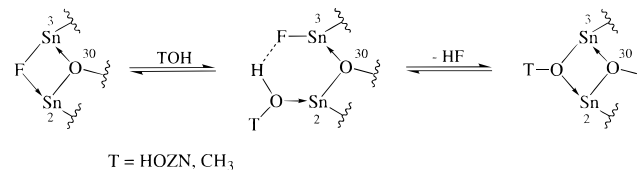
The two high-field methyl  $^1\text{H}$  resonances of  $\text{Me}_2\text{Sn}(2)$  and  $\text{Me}_2\text{Sn}(3)$  split into doublets due to a  $^3J(^1\text{H}-^{19}\text{F})$  of 3 Hz self-consistently confirm the structure characterization of **4**.

**Solution Chemistry.** In order to assess the stability of **4** and its reactivity toward weak hydroxylated nucleophiles, several reactions *in situ* have been monitored by  $^{119}\text{Sn}$  and  $^{19}\text{F}$  NMR.

The minor species obtained upon dissolution of **4** have been identified through their  $^{119}\text{Sn}$  chemical shifts as being **2b** (12%) and **2a** (5%).<sup>1b</sup> However,  $^1\text{H}$  and  $^{119}\text{Sn}$  spectra do not change significantly upon aging, which suggests that equilibrium solutions of **4**, **2a**, and **2b** are stable as compared to similar solutions of the other dimethyltin salicylaldoximates like **2b** and **3**.<sup>1b</sup>

Addition of water to a solution of **4** induces an increase not only of the **2a** but also of the **2b** fraction, while **4** remains the major species. This result confirms the earlier observation that a  $\mu_2$ -hydroxy group bridging Sn(2) and Sn(3) tin atoms is not very stable, **2a** being decomposed to yield **2b**.<sup>1</sup>

Addition of a 10-fold excess of salicylaldoxime to a benzene solution of **4** induces a small increase of the **2b** fraction and several interesting changes in the patterns of the  $^{119}\text{Sn}$  NMR spectrum, though, nevertheless, **4** remains the major species. First, while the Sn(1) chemical shift remains rather unaffected around -444 ppm, a clear deshielding of both Sn(3) and Sn(2) occurs up to -96 ( $\Delta\delta \sim 10$  ppm) and -109 ppm ( $\Delta\delta \sim 11$  ppm), respectively. Second, their  $^1J(^{119}\text{Sn}-^{19}\text{F})$  coupling splitting drops to 1220 and 1150 Hz, respectively, the  $^1J(^{119}\text{Sn}-^{19}\text{F})$  splitting of Sn(1) being almost unchanged around 62 Hz. These values are confirmed by the  $^{19}\text{F}$  NMR spectrum. Third, a dramatic increase of the  $^{119}\text{Sn}$  linewidth is observed for Sn(2) and to a much lesser extent for Sn(1), while that of Sn(3) remains unchanged. These observations are interpreted as

**Scheme 2**

follows. The equilibrium between **4** and **2b** is slow on the  $^{119}\text{Sn}$  NMR time scale, since both present narrow signals in the  $^{119}\text{Sn}$  spectrum. In the presence of a large excess of salicylaldoxime, however, an obvious weakening of the Sn(2)-F bond is observed, as shown by the decrease of the  $^1J(^{119}\text{Sn}-^{19}\text{F})$  scalar splitting and by the linewidth increase of the  $^{119}\text{Sn}(2)$  resonance. Thus, under these experimental conditions, the  $^{119}\text{Sn}$  resonances of **4** enter into pre-coalescence with those of a transient species in which the Sn(2) is no longer bound to fluorine, the  $^{119}\text{Sn}(2)$  resonances of both species becoming averaged. The  $^{119}\text{Sn}(2)$  deshielding is characteristic of a five-coordinate tin atom with a weakened bond. This implies that, in this transient, Sn(2) is bound to another donor species. That the Sn(1) and Sn(3) resonance features are changed to a much lesser extent means that their chemical environments in **4** and in the transient species are rather similar. These observations enable us to propose a transient where Sn(3) is linked to F and Sn(2) is linked to the oximic oxygen of the free salicylaldoxime, as an intermediate on the pathway from **4** to **2b**. This behavior is illustrated in Scheme 2.

As noted, Sn(3) bears a nonbridging fluorine in the transient proposed. Accordingly, the associated effective  $^1J(^{119}\text{Sn}-^{19}\text{F})$  coupling constant should be larger than that measured for Sn(3) in **4**. Consequently, the  $^1J(^{119}\text{Sn}(3)-^{19}\text{F})$  coupling splitting should increase, whereas, experimentally, it decreases. In fact, for the substitution to occur, the acidic hydrogen of the entering nucleophilic oxygen must be transferred to the fluorine atom. The resulting H $\cdots$ F hydrogen bridge should therefore weaken the Sn(3)-F bond, explaining the apparent  $^1J(^{19}\text{F}-^{119}\text{Sn}(3))$  splitting lowering rather than increase expected for a pure Sn-F bond. The latter bridge eventually leads to the formation of HF, as evidenced by a very broad  $^{19}\text{F}$  resonance appearing in the range -100 to -120 ppm, depending on sample nature and concentration.

In order to obtain further experimental support for this interpretation, we repeated the experiment with methanol added in increasing amounts to a benzene solution of **4** (from 0.2 to 10 equiv) and monitored the resulting chemical changes by  $^{119}\text{Sn}$  and  $^{19}\text{F}$  NMR. Increasing the amount of methanol induces an increase in the fraction of **3** in the mixture, paralleled by the decrease of the fractions of **4** and **2b** generated upon dissolution. The latter becomes undetectable after addition of 1.3 equiv of methanol, whereas the residual  $^{119}\text{Sn}$  signal of **4** is still present, even after adding a 10-fold excess of methanol. In addition to the decrease of  $^{119}\text{Sn}$  resonances of **4**, resonance pattern changes as for the reaction between **4** and salicylaldoxime are observed. While the presence of methanol does not affect the  $^{119}\text{Sn}$  tin atom chemical shifts of **4** within  $\pm 1$  ppm, the evolution of the

$^1J(^{119}\text{Sn}-^{19}\text{F})$  coupling splittings and the line shape again depend on the tin atom considered. The apparent  $^3J(^{119}\text{Sn}(1)-^{19}\text{F})$  splitting is insensitive to the presence of methanol, as assessed by  $^{19}\text{F}$  NMR. This indicates the  $^{19}\text{F}$  resonances arise essentially from residual **4**. However, the  $^{119}\text{Sn}(1)$  resonance broadens and finally disappears into the baseline when 6.4 equiv of methanol is added. The  $^1J(^{119}\text{Sn}(3)-^{19}\text{F})$  coupling splitting is only slightly sensitive to the amount of methanol, decreasing from 1271 to 1244 Hz upon addition of 10 equiv of alcohol. The  $^{119}\text{Sn}(3)$  linewidth is totally unaffected during this process. Lastly, the linewidth of the  $^{119}\text{Sn}(2)$  resonance increases while the  $^1J(^{119}\text{Sn}(2)-^{19}\text{F})$  coupling splitting drops from 1285 to 1178 Hz when 6.4 equiv of methanol is added. Beyond this limit, the  $^{119}\text{Sn}(2)$  NMR signal completely vanishes into the baseline. It is obvious that these features result from a dynamic exchange process similar to that for the reaction with salicylaldoxime. Since, on the other hand, the  $^{119}\text{Sn}$  resonances of **3** are perfectly defined in the spectrum, it appears that the interconversion between **4** and **3** obeys likewise the mechanism of Scheme 2.

## Conclusion

This work demonstrates three novel features with regard to  $\mu_2$ -nucleophile bridging tris(diorganotin) disalicylaldoximates. First, the  $\mu_2$ -bridging nucleophile does not need to contain an oxygen, as a  $\mu_2$ -fluoride anion can likewise be incorporated. Second, in contrast with that of the  $\text{Sn}(2)-\text{O}-\text{Sn}(3)$  functionality, the nucleophilic substitution ability of the  $\text{Sn}(2)-\text{F}-\text{Sn}(3)$  functionality decreases in the order  $\text{Me}-\text{OH} > \text{H}-\text{OH} > \text{HOZN}-\text{OH}$ . Third, and most important, for the first time, a mechanism for the peculiar  $\mu_2$ -nucleophilic substitution on the  $\text{Sn}(2)-\text{X}-\text{Sn}(3)$  moiety can be proposed. Thus, for the  $\text{Sn}(2)-\text{F}-\text{Sn}(3)$  moiety, the entering nucleophile  $\text{T}-\text{O}-\text{H}$  causes the cleavage of the  $\text{Sn}-\text{F}$  bond, giving rise to an addition intermediate containing both the  $\text{Sn}(2)-\text{O}(\text{H})\text{T}$  and the  $\text{Sn}(3)-\text{F}$  functionalities, most likely stabilized by the hydroxylic proton of the entering group acting as a hydrogen bridge between the  $\text{TOH}$  oxygen and the fluorine atoms. Subsequently, an intramolecular attack of the entering nucleophile lone pair on the  $\text{Sn}(3)$  atom results in the fluorine leaving, probably as  $\text{HF}$ , and in the formation of a new bridge between  $\text{Sn}(2)$  and  $\text{Sn}(3)$  involving the oxygen of the entering nucleophile. Hence, overall, the  $\mu_2$ -nucleophilic substitution is to be viewed as an addition-elimination reaction. Noteworthy is that the present  $\mu_2$ -F-bridged complex appears to be the most stable one among all the salicylaldoximate complexes synthesized so far.

## Experimental Section

**NMR Experiments.** The samples were prepared by dissolving *ca.* 40 mg of product in 0.5 mL of  $\text{C}_6\text{D}_6$ . All spectra were recorded at 303 K.  $^1\text{H}$ ,  $^{13}\text{C}$ , and  $^{119}\text{Sn}$  NMR spectra were recorded on a Bruker AMX500 spectrometer equipped with a digital lock and operating at 500.13, 125.77, and 186.50 MHz, respectively.  $^{19}\text{F}$  spectra were recorded on a Bruker AC250 spectrometer at 235.35 MHz. NMR data in  $\text{C}_6\text{D}_6$ : chemical shifts in ppm; coupling constants in Hz. The  $^{119}\text{Sn}$  reference frequency was calculated from the absolute frequency of  $\text{Me}_4-$

$\text{Sn}$ ,  $\Xi = 37.290\,665$  MHz.<sup>8</sup> For the  $^{19}\text{F}$  nucleus,  $\Xi = 94.094\,003$  MHz.<sup>8b</sup>  $^{13}\text{C}$  and  $^1\text{H}$  chemical shifts were referenced to the solvent ( $\text{C}_6\text{D}_6$ )  $^{13}\text{C}$  resonance at 128.0 ppm and to the residual solvent ( $\text{C}_6\text{D}_5\text{H}$ )  $^1\text{H}$  resonance at 7.15 ppm, respectively. Multiplicity patterns in  $^1\text{H}$ ,  $^{119}\text{Sn}$ , and  $^{13}\text{C}$  spectra: d, doublet; dd, doublet of doublets; ddd, doublet of doublets of doublets; s, singlet; m, complex pattern; nr, nonresolved.  $^nJ(^1\text{H}-^1\text{H})$  coupling constants are given within brackets.  $^3J(^1\text{H}-^{19}\text{F})$ ,  $^2J(^{13}\text{C}-^{19}\text{F})$ , and  $^1J(^{119}\text{Sn}-^{19}\text{F})$  are mentioned explicitly.  $^nJ(^1\text{H}-^{119}\text{Sn})$ ,  $^1J(^{13}\text{C}-^{119/117}\text{Sn})$ , and  $^2J(^{119}\text{Sn}-^{119/117}\text{Sn})$  coupling constants are given in Table 1 and not repeated here.

Broad-band  $^1\text{H}$ -decoupled  $^{13}\text{C}$  and  $^{119}\text{Sn}$  spectra were recorded using Bruker standard pulse sequences. All heteronuclear correlation spectroscopy experiments consisted of gradient-enhanced versions of the standard  $^1\text{H}-^{119}\text{Sn}$  HMQC and  $^1\text{H}-^{13}\text{C}$  HMQC or HMBC pulse sequences, implemented in exactly the same way as explained elsewhere and processed in the magnitude mode.<sup>1b</sup>

**Syntheses. Compound 2b.** Compound **2b** was synthesized as previously described.<sup>1b</sup>

**Compound 4.** To a solution of 10 g (11.5 mmol) of **2b** in 170 mL of dichloromethane was added 513 mg (13.8 mmol, 1.2 equiv) of ammonium fluoride. The mixture was refluxed for 3 h with magnetic stirring under a dry atmosphere. After filtration of the unreacted ammonium fluoride, the solvent was evaporated to yield 10.03 g of a crude solid mixture of **4**, **2b**, and salicylaldoxime. This mixture was stirred in refluxing hexane (360 mL) for 3 h. The undissolved fraction was filtered off, and the filtrate was concentrated at 50 °C, under vacuum, to one-third of its initial volume. When the concentrate was cooled to room temperature, an oil separated from the mixture. The supernatant hexane solution isolated was then cooled at 5 °C for 48 h. Recrystallization in hexane of the precipitate obtained provided 1.36 g of pure **4** (yield: 16%).

The analytically pure crystals of **4** began decomposing above 100 °C prior to melting.

**Characterization.** Anal. Calc for  $\text{C}_{20}\text{H}_{29}\text{O}_5\text{N}_2\text{F}_3\text{Sn}_3$  ( $M = 752.53$ ): C, 31.9; H, 3.9; N, 3.7. Found: C, 32.4; H, 4.1; N, 3.7.  $^1\text{H}$  NMR ( $\text{C}_6\text{D}_6$ , 250 MHz): 13.55 s OH(9); 8.17 s H(17); 8.10 s H(7); 7.06–7.02 nr H(3') and H(4'); 6.94 ddd [8.2, 7.2, 1.9] H(4); 6.80 dd [7.7, 1.8] H(6); 6.78 ddd [7.1, 1.7, 1.7] H(6'); 6.60–6.53 nr H(5) and H(5'); 6.12 d [8.1] H(3); 1.07 s  $\text{CH}_3$  (Sn(1)); 0.60 d,  $^3J(^1\text{H}-^{19}\text{F}) = 3.3$ ,  $\text{CH}_3$  (Sn(2)); 0.55 d,  $^3J(^1\text{H}-^{19}\text{F}) = 3.2$ ,  $\text{CH}_3$  (Sn(3)).  $^{13}\text{C}$  NMR ( $\text{C}_6\text{D}_6$ , 62.9 MHz): 162.4 C(2'); 160.4 C(2); 155.6 C(17); 150.0 C(7); 135.6 C(6); 132.8 C(4'); 132.4 C(6'); 131.3 C(4); 120.9 C(3'); 120.5 C(1); 118.9 C(1'); 117.7 C(5); 117.5 C(3) and C(5'); 14.8 C(Sn1); 2.9 d,  $^2J(^{13}\text{C}-^{19}\text{F}) = 16.9$ , C(Sn2); 0.9 d,  $^2J(^{13}\text{C}-^{19}\text{F}) = 16.1$ , C(Sn3).  $^{19}\text{F}$  NMR ( $\text{C}_6\text{D}_6$ , 235.35 MHz): –83.9.  $^{119}\text{Sn}$  NMR ( $\text{C}_6\text{D}_6$ , 186.50 MHz): –105.7 d,  $^1J(^{119}\text{Sn}-^{19}\text{F}) = 1271$ , Sn(3); –120.3 d,  $^1J(^{119}\text{Sn}-^{19}\text{F}) = 1285$ , Sn(2); –444.6 d,  $^3J(^{119}\text{Sn}-^{19}\text{F}) = 65$ , Sn(1).

**Acknowledgment.** Financial support of the Fund for Scientific Research, Flanders, Belgium (FKFO; Grant No. 2.0094.94), and of the Belgian Nationale Loterij (Grant No. 9.0006.93) is gratefully acknowledged (R.W., M.B.). We thank Mrs. I. Verbruggen for recording routine NMR spectra. A postdoctoral grant from the Fund for Scientific Research, Flanders, Belgium (Grant No. V10/6-AB-D12073), is gratefully acknowledged (A.M.).

IC970866E

- (8) (a) Davies, A. G.; Harrison, P. G.; Kennedy, J. D.; Puddephatt, R. J.; Mitchell, T. N.; McFarlane, W. *J. Chem. Soc. A* **1969**, 1136. (b) Mason, J. *Multinuclear NMR*; Plenum Press: New York, 1987; pp 625–629.